

1 **Tungsten Thermionic Emission as a Gauge for Low Pressures of**
2 **Cesium Vapor**

3 João F. Shida,^{*} Fangjian Wu,[†] and Eric Spieglan[‡]

4 *Physics Department and Enrico Fermi Institute,*
5 *The University of Chicago, Chicago, IL, 60637*

6 Mesut Çalışkan[§]

7 *Physics Department and Kavli Institute for Cosmological Physics,*
8 *The University of Chicago, Chicago, IL, 60637*

9 (Dated: September 3, 2020)

10 **Abstract**

11 Heated metal filaments under electric fields and low pressures of alkali metal gas eject electrons
12 by thermionic emission as a function of the pressure of the gas and the temperature of the filament.
13 To explore this process in a program to develop large-area alkali metal photocathodes, we have
14 designed and built a gauge following the studies of Taylor and Langmuir^{1,2}. We present proof-
15 of-principle measurements of the thermionic emission of a tungsten filament in cesium vapor. We
16 describe a second generation design that corrects flaws in the first gauge.

17 **I. INTRODUCTION**

18 Alkali metals adsorb onto metal surfaces, with a concentration and structure dependant
19 on the temperature of the surface and the pressure of the metal vapor. The adsorption
20 increases the thermionic emission of the surface compared to bare metal. We show that by
21 measuring the thermionic emission as a function of the temperature of a tungsten filament,
22 one can infer the pressure of cesium vapor around the filament.

23 According to Richardson's law, the thermionic current is solely determined by the work
24 function of the surface and its temperature:

$$J = \lambda_R A_0 T^2 e^{-W/k_B T} \quad (1)$$

25 The work function changes with the coverage of adsorbed cesium atoms. For coverages
26 between 0 and 0.66, the adsorbed atoms lose an electron, creating an ionic charge layer
27 which diminishes the work function and increases thermionic emission³.

28 For coverages above 0.66, the work function is low enough so that cesium ions that adsorb
29 do not lose an electron, creating a neutral layer. To accommodate the larger radius of the
30 neutral atoms, this layer is rotated 30 ° about the normal⁴ relative to the ionized layer below.
31 The work function approaches that of cesium metal, suppressing thermionic emission.

32 Taylor and Langmuir^{2,5} describe a relationship between the temperature of a tungsten
33 filament, the cesium vapor pressure, and tungsten thermionic emission. The dotted curves
34 in Fig. 1 show the relationship of the thermionic emission as the temperature of the filament
35 changes for different cesium atom fluxes, and is reproduced from Fig. 15 in their 1933 paper².

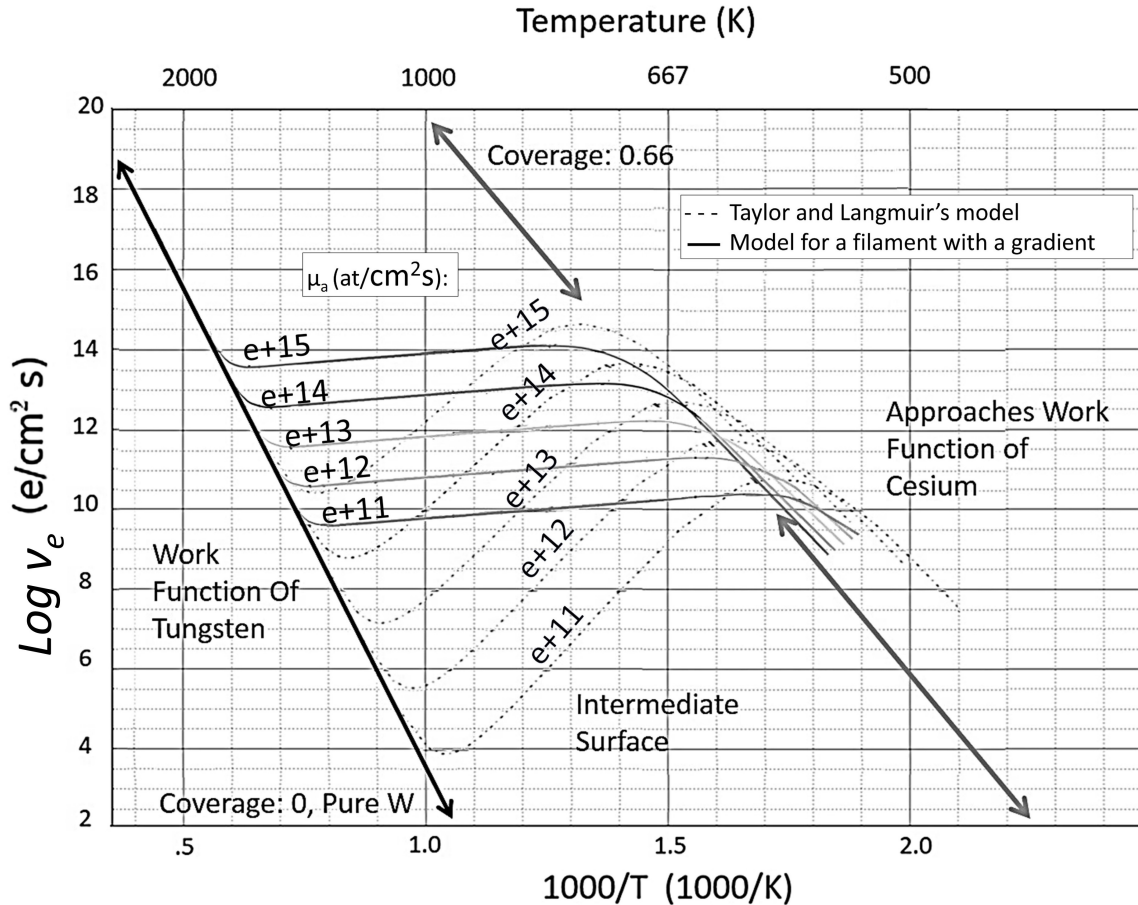


FIG. 1. The electronic thermionic emission calculated with Taylor and Langmuir's measurements is shown as dotted lines for 5 atom flux values of cesium proportional to vapor pressures (indicated on top of the curves, e.g. e+11). To account for the thermal gradient of the filament in our gauge, we have corrected the Taylor and Langmuir model by integrating over the filament, with the result shown as solid lines. The features of the curves such as the peaks and valleys become flattened with a filament that has a temperature gradient: The hotter central parts of the filament emit orders of magnitude less electrons than the colder edges of the filament, which obscures the emission of the center and flattens the valley of the curve. The y-axis indicating thermionic emission is in log scale.

36 As an educational sidebar in a program to develop large-area alkali metal photocathodes,
 37 we have explored thermionic emission by building a gauge to measure the partial pressure
 38 of cesium in the pressure range between 10^{-5} and 10^{-3} Pa. Section II describes the gauge
 39 construction, assembly and operation. The results are presented in the context of the Taylor

40 and Langmuir model in Section III. Section IV describes lessons we have learned from this
 41 first generation gauge, and describes specific solutions to issues we encountered.

42 II. GAUGE ASSEMBLY AND OPERATION

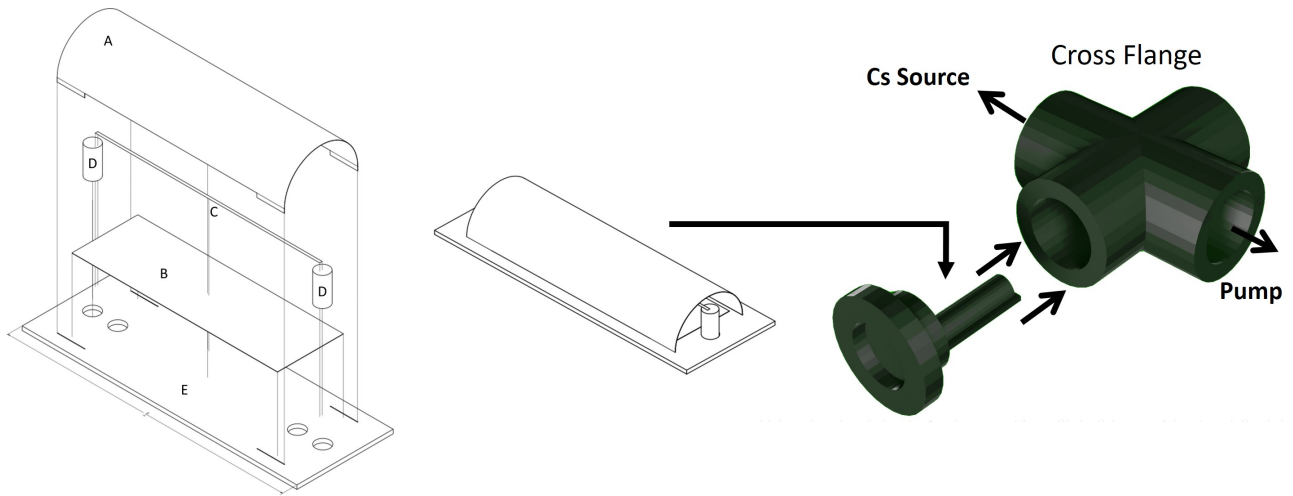


FIG. 2. On the left, the exploded assembly of the gauge, on the middle, the assembled gauge, and on the right the positioning of the gauge in the manifold. There are copper wires that were not depicted connecting the cylindrical (A) and flat (B) copper plates, as well as the filament ends, to independent pins in a feedthrough. The filament (C) is connected to screws which act as leads (D). All elements are isolated from each other through ceramic beads and boards like the base ceramic support (E). The copper wires are thick enough to support the structure without it dipping and touching the manifold.

43 The proof-of-concept gauge is shown in Fig. 2. It consists of a tungsten ribbon filament
 44 surrounded by a collector for the thermionic current. The collector comprises a flat base
 45 made with a ceramic rectangular plate coated with copper, on which is mounted a semi-
 46 cylindrical copper sheet. The tungsten ribbon is supported on the rectangular plate by
 47 isolating screws at each end which serve as terminals for the filament. All components are
 48 inside a 2 3/4" CF 4-way cross flange, and are individually connected by ceramic-isolated
 49 copper wires to a vacuum feedthrough at one end of the cross. The CF cross connects to
 50 a valve leading to a custom cesium source containing a glass vial of pure cesium⁶, and also
 51 connects to a turbo pump. After the system was pumped to a pressure in the order of

52 1.3×10^{-5} Pa , the vial was broken to introduce the cesium to the system⁷. The pump was
53 valved off during measurements.

54 Thermal control of the manifold is necessary to achieve temperature uniformity and
55 control cold spots in the manifold where cesium vapor could condense. The manifold is
56 surrounded by K-type thermocouples and heaters, which are covered by fiberglass insulation.
57 The temperature of the cesium source was varied to check the measurements from the gauge
58 against the calculated pressure.

59 The circuit used to measure thermionic emission is outlined in Fig. 3. It comprises two
60 subsystems, the heating of the filament, and collectors that measure thermionic emission.
61 The heating circuit consists of a power supply with built-in ammeter and voltmeter (A and
62 V in Fig. 3) connected to the screws at the ends of the tungsten filament, with the negative
63 terminal set at manifold ground. The measurement circuit consists of the copper plate and
64 semi-circular sheet collectors tied to a bias voltage relative to ground through a 10.03 k Ω
65 resistor. The voltage from the collector current, typically 0.01 - 100 V, is measured across
66 this resistor.

67 As the bias voltage increases from zero more thermionic electrons are directed to the
68 collectors. There is a critical bias voltage after which the current plateaus because all
69 emitted electrons reach the filament. We reproduced Fig. 21 in the Taylor and Langmuir
70 paper² to find this point, 180 - 200 V, as shown in Fig. 4. All measurements were performed
71 at or beyond this critical bias voltage.

72 A measurement with the gauge consists of changing the the filament temperature by
73 changing the current, and measuring the collection current by the voltage through the 10.03
74 k Ω resistor. The collected electron current divided by the surface area of the filament
75 yields the thermionic electron flux. The conversion between filament current to filament
76 temperature invokes a temperature transport equation, as described in Appendix A.

77 The measurements can be fit to the model of Taylor and Langmuir, which is used to infer
78 the flux of cesium atoms in the manifold, and hence the Cs partial pressure. Measurements
79 were taken without the aid of automated logging using voltmeters with 0.01 V precision.
80 An automated measurement algorithm could easily be implemented.

81 Before each measurement the circuit was probed for shorts between circuit elements
82 and/or ground from cesium condensation on the gauge surfaces. To eliminate the shorts,
83 we applied 300 V between each element and between the elements and ground. The initial

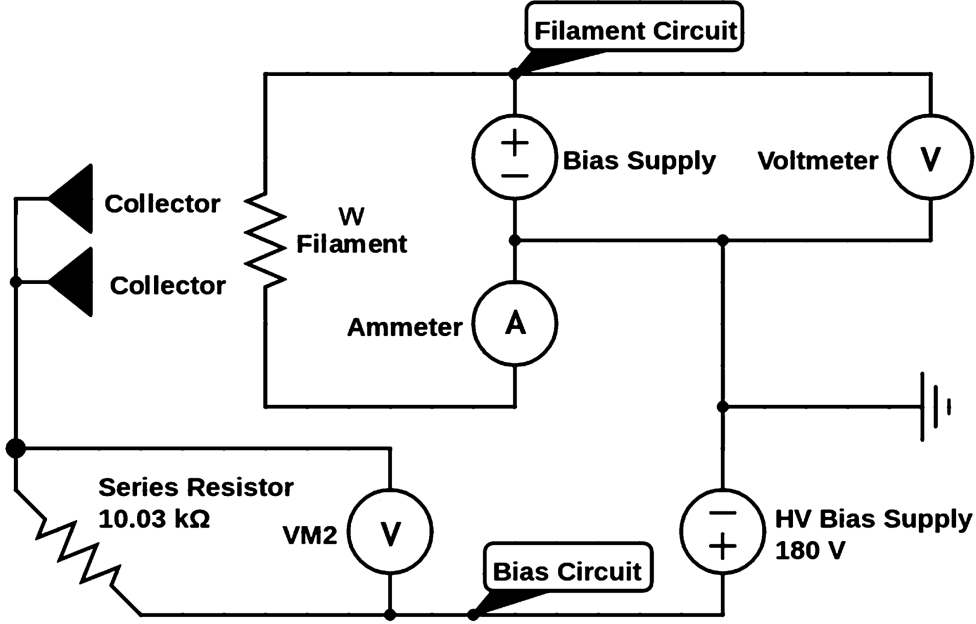


FIG. 3. Circuitry of the gauge. Thermionic electrons leave the filament at ground voltage and are pulled by an electric field towards the collectors at a high voltage (>200 V+). They then pass through the series resistor and the voltage is voltmeter 2 is proportional to the thermionic emission from the filament.

84 low resistances increased to over 10 k Ω once the bias was applied. If the system was left
 85 idle for more than two hours, even if heated, the shorts returned and the process had to be
 86 repeated.

87 III. RESULTS AND DISCUSSION

88 Measurements of thermionic emission were taken at source temperatures of 363 K (Mea-
 89 surement A) and 305 K (Measurement B) with the manifold temperatures at 503 K and 516
 90 K, respectively. The measured pressures fit to 1.30×10^{-4} and 8.34×10^{-4} Pa as shown in Fig.
 91 5. As expected, thermionic emission is greater at higher source temperatures. The results
 92 match a pure tungsten curve at high filament temperatures.

93 The measured data do not match Taylor and Langmuir's (TL) predictions. The filament
 94 we used had a temperature gradient due to thermal conduction at the leads. In contrast, the
 95 TL results were obtained by using guard rings to suppress collection from filament segments

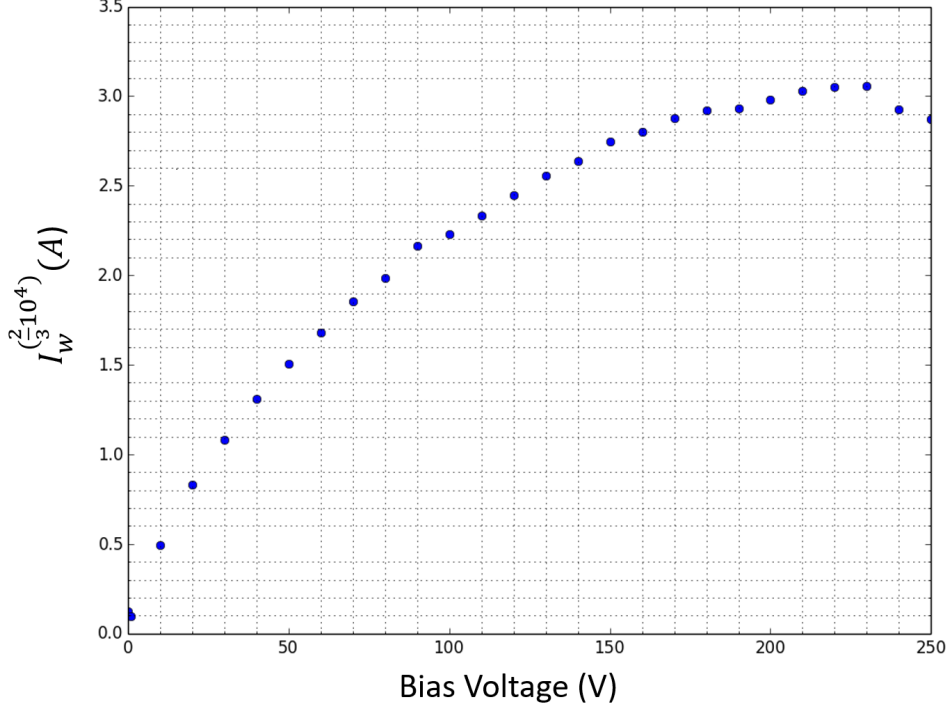


FIG. 4. Curve of measured thermionic current versus increased bias voltage (difference between collectors and filament). In this case the critical voltage observed was around 200V and after that the collected current started plateauing. If measurements were taken at a voltage before the plateau, not all electrons would be collected for some temperatures of the filament which would indicate a lower pressure. The current was manipulated as the y-axis indicates to be in the same form as Fig. 21 in the Taylor and Langmuir paper².

96 that were not uniform in temperature: electronic thermionic emission was nearly uniform
 97 along the fraction of the filament measured. A correction based on the temperature gradient
 98 was computed, described in Appendix A. The corrected curve can be seen in Fig. 1 as the
 99 solid lines, and in Figs. 5,6. The corrected model agrees much better with the data.

100 At filament temperatures decrease towards that of the manifold, heat conduction into
 101 the filament becomes significant, altering the relationship between filament current and
 102 temperature. The gauge was operated at elevated temperatures (>200 °C, above 500 K for
 103 the measurements) to minimize cesium condensation; results at filament temperatures close
 104 to that of the manifold are omitted.

105 The proof-of-principle gauge failed after commissioning and two series of measurements

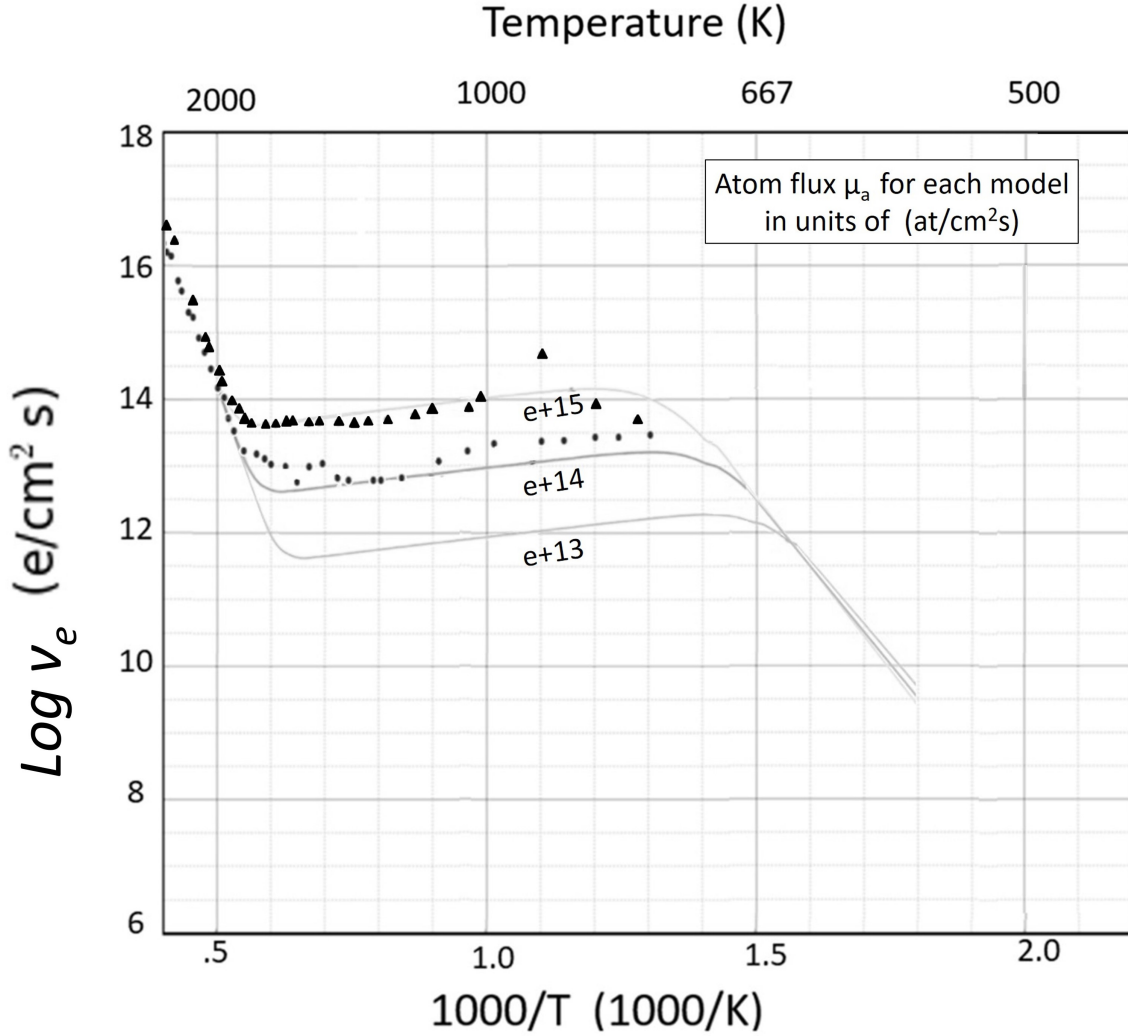


FIG. 5. The logarithm of Thermionic emission as measured by the gauge versus 1000/Filament Temperature for two measurements. Measurement A (triangles) was taken at a higher partial pressure of cesium than measurement B (circles), with the cesium source temperatures being 363K and 305K respectively. The outlier in measurement A is most likely a mistake.

106 due to cesium condensation impervious to evaporation. After the system had been opened
 107 and exposed to air, we verified a darkening of essentially all ceramic surfaces. Between
 108 electronic terminals, lighter patches appeared. This coloration pattern can be explained by
 109 cesium deposition and later vaporization between electronic terminals. When exposed to
 110 air, remaining cesium darkened. For a more in-depth discussion on operation precautions
 111 and leakage currents, see Appendix B.

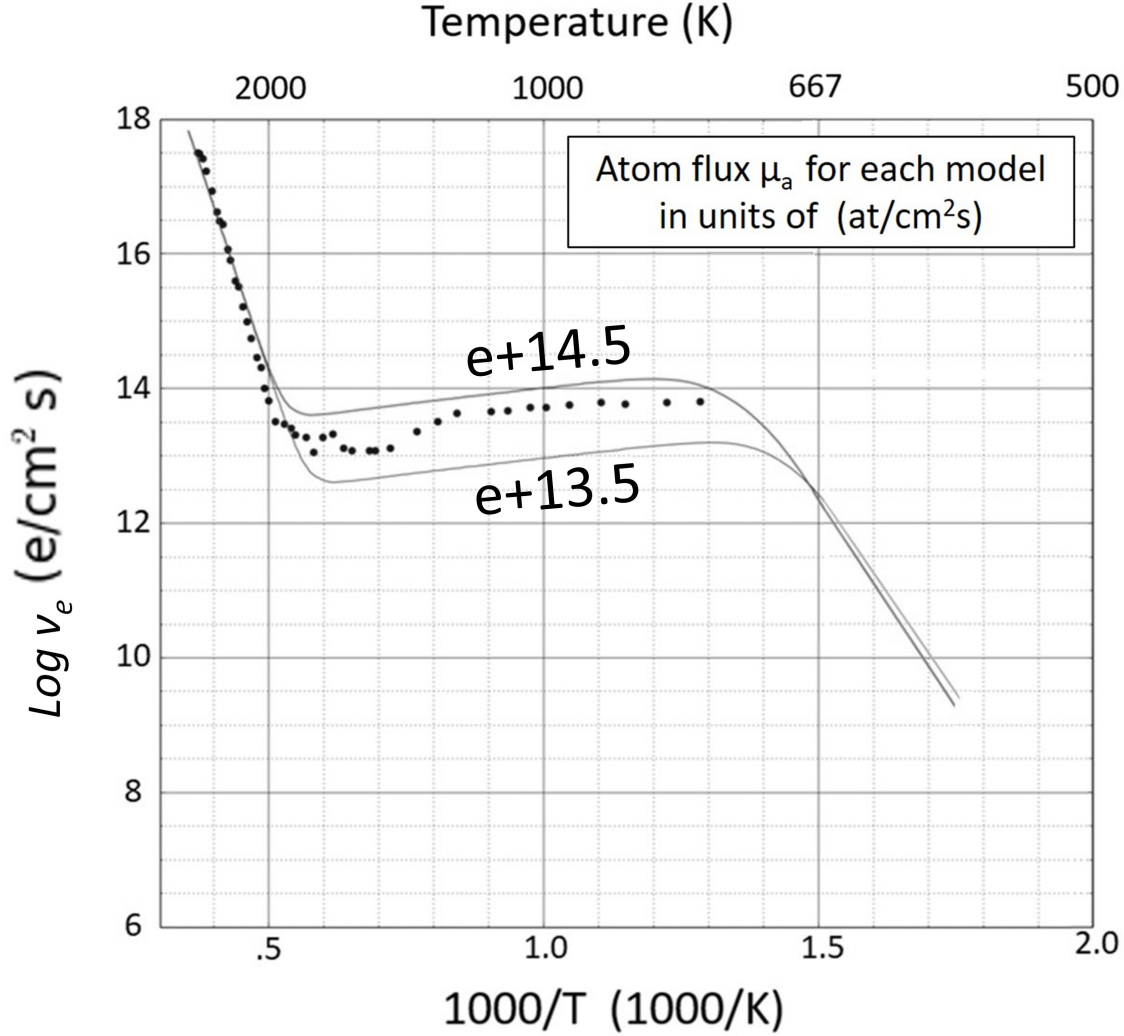


FIG. 6. One measurement of the thermionic emission curve as a function of temperature. This measurement is fit to a solid curve corresponding to $10^{14.23} \text{at/cm}^2 \text{s}$, an atom flux which can be converted to $1.30 \times 10^{-4} \text{ Pa}$. The y-axis is in Log scale.

112 IV. LESSONS LEARNED: PROPOSED SECOND GENERATION GAUGE

113 The proof-of-concept gauge demonstrated the Taylor and Langmuir model can be used
 114 to measure cesium pressures, but made apparent that we had made mistakes in the design.
 115 The condensation of cesium vapor shorting circuit elements, and the presence of a filament
 116 temperature gradient are the main issues. An example second-generation instrument is
 117 illustrated in Fig. 7 and described in Subsection A. Alternatively, Springer and Cameron
 118 had proposed another method using a Bayer-Alpert gauge to measure partial pressures of

119 cesium using its ions instead of electrons^{8,9}, as described in Subsection B.

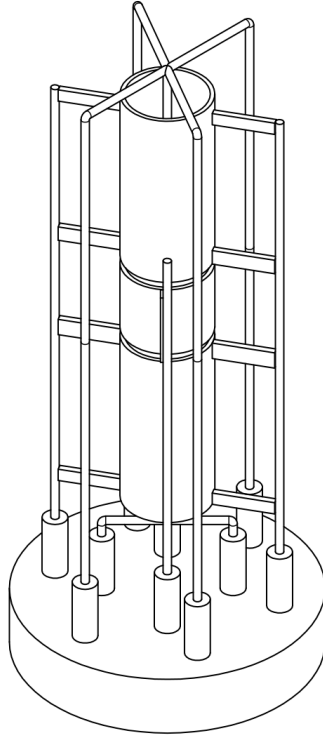


FIG. 7. A scheme for a possible gauge redesign based on the results of the proof-of-concept gauge and its shortcomings. This design includes guard rings and minimizes structural-nonconducting surfaces to avoid leakage currents and improve signal.

120 **A. Improved gauge using thermionic emission**

121 In order to counter leakage currents and electrical shorts, the gauge must minimize areas
122 for cesium deposition around relevant conductors such as the collector or the leads. All
123 circuit elements must avoid contact with support structures if possible. One solution is to
124 have the circuit elements be self-supporting as in Fig. 7.

125 To account for the filament temperature gradient, the collector may be split into two
126 guard rings and a central collector ring (Fig. 7, Fig. 8). All rings should be cylindrical and
127 biased at the same voltage to create a uniform radial electric field. Only the central guard
128 ring would be used to measure thermionic emission as the center is the hottest part of the
129 filament with the smallest gradients. This was done by Taylor and Langmuir².

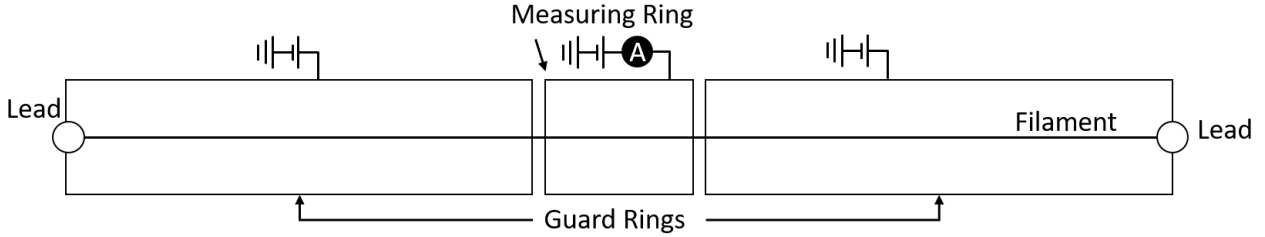


FIG. 8. A scheme for how guard rings and the measurement conductor would be arranged. All three conductors would be biased at the same voltage and have the same shape. Around the center of the filament, the temperature can be considered almost constant. This means that instead of a flattened curve, we would measure the same curve Taylor and Langmuir predict. Cylinders attached to the base are made of ceramic/insulating material, but all other elements are metal. It is paramount that the setup is structurally rigid to avoid shorts from small mechanical impacts/deformations.

130 The effectiveness of the guard rings is improved if the ends of the filament are coiled,
 131 increasing the length of the filament and thus flattening the temperature gradient. Although
 132 the emissions from the coiled areas will not follow the Taylor and Langmuir model, they will
 133 be shielded by the guard rings and not measured by the central ring.

134 B. Using ionized cesium over electrons as an alternative

135 An alternative method is to measure the current of ionized cesium ions instead of electrons
 136 thermionically emitted from the metal surface. A commercial Bayard Alpert gauge (BAG)
 137 is an ion gauge with an emitter filament, a collector filament a cylindrical grid along the
 138 collector length. Springer and Cameron heated the grid to eject electrons and ionize cesium
 139 and biased the collector filament negatively to collect the ions. Measuring the collected
 140 current yields the cesium partial pressure in a similar way to the method described in this
 141 paper.

142 We had originally intended for the proof-of-principle gauge to be usable in ionic and
 143 electronic regimes. However, given the difficulties with cesium condensation the electron
 144 regime was preferred.

145 V. CONCLUSION

146 From the relationship between the thermionic emission of a tungsten filament and its
147 temperature in the presence of cesium vapor, a gauge can be built to determine the partial
148 pressure of the cesium. We have shown a proof-of-concept gauge and measurements, doc-
149 umented its problems, and proposed a new design. We hope this paper is useful to those
150 who wish to construct a similar device, or to explore the principles of thermionic emission,
151 metallic crystal growth on metal surfaces, and work-functions.

152 ACKNOWLEDGMENTS

153 The authors would like to thank (Dr.) Evan Angelico, Andrey Elagin, Henry Frisch and
154 Mary Heintz for their help during the project; Matthew Poelker and Charles Sinclair for their
155 insightful comments and helpful suggestions. We also thank Nicole Dombrowski, Hayward
156 Melton and Hannah Tomlinson for their previous work on assembling the proof-of-concept
157 gauge.

158 VI. APPENDIX A: CALCULATIONS FOR WIRE TEMPERATURE GRADIENT

159 To obtain the partial pressure of cesium, we must produce an experimental curve of
160 thermionic emission versus temperature of the filament. To do so it is necessary to convert
161 the two observable parameters, the current through the tungsten filament (I_w) and the
162 current observed entering collecting conductors (I_c) to the temperature of the filament (T_w)
163 and to the number of electrons leaving the filament (ν_e) respectively.

164 The temperature of the filament is paramount to the characterization of the thermionic
165 current. In their experiments, Taylor and Langmuir made use of guard rings to only measure
166 thermionic electrons from the very center of their filaments so that they may safely assume
167 its temperature is uniform in that region. However, without using guard rings, and instead
168 measuring electrons from the entire length of the filament, it is necessary to account for the
169 filament's temperature gradient.

170 Since the leads conduct heat away from the filament, there is a temperature gradient with
171 a peak at the midpoint. The equation that represents the equilibrium (a steady temperature

172 distribution) for a small part of the filament is:

$$0 = dPe + dPti - dPi - dPto \quad (2)$$

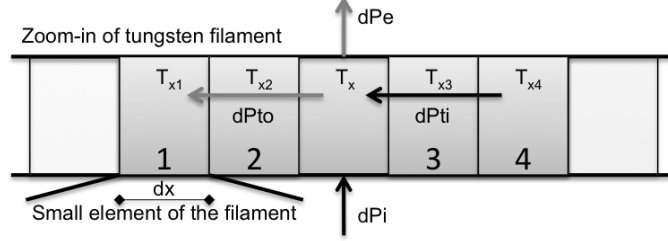


FIG. 9. Power transport scheme for a small piece of the filament, the different pieces are numbered as they are used in the equations 3 to 10. The Black arrows indicate power into the filament piece, and the grey arrows indicate power out. $dPti$ is the power piece 3 conducts from piece 4 into the center piece, and $dPto$ is the power piece 2 conducts from the center piece to piece 1.

173 Where dPe is the power lost by emission, dPi is the power from the current through
 174 the filament, $dPti$ is the power conducted in from the hotter end and $dPto$ is the power
 175 conducted out at the colder end (see Fig. 9). Each of these components can be written out
 176 as a function of the position in the filament as follows:

$$dPe = dA_e \epsilon_{(T(x))} \sigma T(x)^4 \quad (3)$$

$$dPi = \frac{i^2 \rho_{(T(x))} dx}{A_t} \quad (4)$$

$$dPti = A_t K_{(T(x_3))} \frac{T_{(x_4)} - T_{(x)}}{dx} \quad (5)$$

$$dPto = A_t K_{(T(x_2))} \frac{T_{(x)} - T_{(x_1)}}{dx} \quad (6)$$

180 Where l, w and d are the dimensions of the filament, with l being its long edge, A_e is the
 181 external area of the filament, A_t is the transverse area of the filament (in our case of a flat
 182 filament, $A_e = 2l(w + d)$ and $A_t = wd$ respectively); σ is the Stefan-Boltzmann constant,
 183 $T_{(x)}$ is the temperature gradient; i is the current through the filament. Furthermore, $\rho_{(T(x))}$
 184 is the resistivity of tungsten as a function of temperature; $\epsilon_{(T(x))}$ is the emissivity of tungsten
 185 as a function of temperature; and $K_{(T(x))}$ is the conductivity of tungsten as a function of
 186 temperature. These three tungsten properties were all fitted to 4th or 5th order polynomials
 187 as a function of T .

188 Note that equations 5 and 6 can be re-written as a function of the first derivative of $T_{(x)}$
 189 at x_3 and x_2 respectively:

$$dPti = A_t K_{(T(x_3))} \frac{dT(x_3)}{dx} \quad (7)$$

$$dPto = A_t K_{(T(x_2))} \frac{dT(x_2)}{dx} \quad (8)$$

191 Substituting equations 3, 4, 7 and 8 back into equation 2 we have:

$$0 = dA_e \epsilon_{(T(x))} \sigma T_{(x)}^4 + \frac{i^2 \rho_{(T(x))} dx}{A_t} + (A_t K_{(T(x_3))} \frac{dT(x_3)}{dx} - A_t K_{(T(x_2))} \frac{dT(x_2)}{dx}) \quad (9)$$

192 Which can also be re-written as a function of the second derivative of $T_{(x)}$:

$$0 = dA_e \epsilon_{(T(x))} \sigma T_{(x)}^4 + \frac{i^2 \rho_{(T(x))} dx}{A_t} + A_t \left(\left(\frac{dT_{(x)}}{dx} \right)^2 \frac{dK_{(T(x))}}{dT_{(x)}} + K_{(T(x))} \frac{dT_{(x)}^2}{d^2x} \right) dx \quad (10)$$

193 This is a second order differential equation that can be solved numerically for T_x with two
 194 boundary conditions. We assume knowledge of the temperature of the ends of the filament,
 195 which is valid if the leads it is connected to are heat-sunk enough to the manifold, the
 196 temperature of which we can measure. Furthermore, given that at high temperatures $K_{(T)}$
 197 is small, we assume that for the very center of the wire, where it is hottest, equation 2 has
 198 negligible conduction summands, and thus we can solve for the temperature at the midpoint
 199 given a current. Therefore, we have both $T_{(0)}$ and $T_{(\frac{l}{2})}$ as boundary conditions. Solving for
 200 $T_{(x)}$ we get, for any current, a temperature gradient in the filament.

201 Once we have $T_{(x)}$, we can perform a numerical integration of how many thermionic
 202 electrons will be emitted by different parts of the filament based on Taylor and Langmuir's
 203 experimentally determined curve. We do this to calculate the predicted thermionic emission
 204 from a filament with non uniform temperatures, and we can generate a curve analogous to
 205 Taylor and Langmuir's but for a filament with a temperature gradient instead of a uniformly
 206 heated filament (See dotted lines in Fig. 1).

207 VII. APPENDIX B: OPERATION PRECAUTIONS

208 A measurement with the gauge has been described above. However, to obtain repro-
 209 ducible results, certain precautions must be taken.

210 Taylor and Langmuir recommend that before any measurement is done the filament
 211 undergoes what they call an aging process. This involves leaving the filament heated at

212 2400K for 10 hours, then at 2600 K for an hour and finally conclude with a few brief
213 flashes at 2900K. Prior to such aging, neither we nor Taylor and Langmuir could obtain
214 reproducible results. Furthermore, we have determined that brief flashes to about 2500K
215 before any measurement generate more reproducible results as well.

216 It is also necessary that the measurement not interfere appreciably with the temperature
217 of the source of cesium. The filament heats up to high temperatures during the measurement
218 (up to 2500 K) and if the cesium source temperature changes mid-measurement, so will the
219 pressure of cesium vapor. A fast measurement can solve this issue, as well as placing the
220 source far away from the filament or using a thinner filament.

221 A. Leakage Current

222 Leakage currents between the charged plates and either ground or the filament terminals
223 increase the background in the measurement of the currents collected from the plates. We
224 attribute this leakage current to condensed cesium on the ceramic tile connecting the ends
225 of the filament, the plates and the manifold together.

226 There are two ways leakage currents interfere with the measurements. It makes it so that
227 the signal measured across the series resistor does not only come from collected thermionic
228 electrons, but also from ground electrons that arrive from leakage conductive paths. Fur-
229 thermore, as one changes the temperature of the conductive paths, cesium evaporates or
230 condenses, thus changing the resistance of the leakage pathways. This means that there is
231 not a simple static current background one might subtract from the measured signal.

232 It is possible to deal with such currents, however. By applying high voltages to the circuit
233 elements any conductive cesium paths to ground will heat up and the cesium will evaporate
234 off the surfaces. For the charged plates, half an hour at 300V took a 10 k Ω short to up
235 to tens of M Ω . Another effective counter to leakage currents was to keep the gauge much
236 hotter than the source to avoid creating sites prone to cesium deposition. When source
237 and manifold were left at the about the same temperature, all of the circuit elements were
238 connected to each other and to ground by resistances under one k Ω . When the manifold was
239 left at a four times the temperature of the source, however, resistances went up to hundreds

240 of $k\Omega$.

241 * joaofshida@uchicago.edu

242 † fjwu@uchicago.edu

243 ‡ eric.spieglan@gmail.com

244 § mesut@uchicago.edu

245 ¹ C. Sinclair, “Alkali Metal Sources for Photocathodes and their Quantification – Getter Sources
246 vs. Metallic Evaporation Sources” presented at the *UChicago Photocathode Workshop*, (2012);

247 ² J.B. Taylor and I. Langmuir, “The Evaporation of Atoms, Ions and Electrons from Caesium
248 Films on Tungsten” in *Physical Review* 44, 423, (1933) ;

249 ³ V. M. Gavriilyuk, A. G. Naumovets, and A. G. Fedorus, “Investigation of adsorption of cesium
250 on a tungsten single crystal” in *J. Exptl. Theoret. Phys. (U.S.S.R.)* 51, 1332-1340, (1966) ;

251 ⁴ A. G. Naumovets and A. G. Fedorus, “Cesium on tungsten (011) face; structure and work
252 function” in *Surface Science Vol. 21, Iss. 2, 426-439*, (1970) ;

253 ⁵ J.B. Taylor and I. Langmuir, “Vapor Pressure of Caesium by the Positive Ion Method” in
254 *Physical Review* 51, 753, (1937) ;

255 ⁶ Cs sample purchased from Alfa Aesar by Thermo Fischer Scientific, (2018);

256 ⁷ E. Angelico, E. Spieglan, A. Elagin, H. Frisch, A. Bernhard, “Dual Low Vacuum-UltraHigh
257 Vacuum System for Large-Scale Production of Micro-Channel Plate Photomultipliers” in *US*
258 *Patent 62928598; filed Oct. 31 (Pending)* (2019);

259 ⁸ R.W. Springer, B.J. Cameron, “Photocathode transfer and storage techniques using alkali vapor
260 feedback control” Presented at *the 13th International Free-Electron Laser Conference, Santa Fe,*
261 *NM, 25-30 Aug. 1991* **92**.

262 ⁹ Private communication with Dr. Charles Sinclair, (2020);

263 ¹⁰ E. Angelico, A. Elagin, H. Frisch, E. Spieglan, B. Adams, M. Foley, M. Minot. “Air-transfer pro-
264 duction method for large-area picosecond photodetectors” in *Review of Scientific Instruments.*
265 91. 053105. (2020) 10.1063/5.0008606.